Article:
Han, Y, Tian, W, Chipperfield, MP et al. (2019) Attribution of the Hemispheric Asymmetries in Trends of Stratospheric Trace Gases Inferred From Microwave Limb Sounder (MLS) Measurements. Journal of Geophysical Research: Atmospheres, 124 (12). pp. 6283-6293. ISSN: 2169-897X

https://doi.org/10.1029/2018JD029723

JGR Atmospheres

RESEARCH ARTICLE
10.1029/2018JD029723

Special Section:
Long-term Changes and Trends in the Middle and Upper Atmosphere

Attribution of the Hemispheric Asymmetries in Trends of Stratospheric Trace Gases Inferred From Microwave Limb Sounder (MLS) Measurements

Yuanyuan Han[1,2], Wenshou Tian[2], Martyn P. Chipperfield[3,4], Jiankai Zhang[2], Feiyang Wang[2], Wenjun Sang[2], Jiali Luo[2], Wuhu Feng[4,5], Andreas Chrysanthou[4], and Hongying Tian[2]

[1]School of Environmental and Chemical Engineering, Xi'an Polytechnic University, Xi'an, China, [2]Key Laboratory for Semi-Arid Climate Change of the Ministry of Education, College of Atmospheric Sciences, Lanzhou University, Lanzhou, China, [3]National Centre for Earth Observation, University of Leeds, Leeds, UK, [4]School of Earth and Environment, University of Leeds, Leeds, UK, [5]National Centre for Atmospheric Science, University of Leeds, Leeds, UK

Abstract Using Microwave Limb Sounder (MLS) satellite observations, ERA-Interim reanalysis data, and a chemistry transport model simulation, we analyze and investigate the causes of the asymmetric hemispheric trends of N_2O, CH_4, and HCl in the stratosphere during the period 2004–2012. We find significant hemispheric asymmetries in the trends of these trace gases in the midlatitude middle and lower stratosphere. With regard to N_2O and CH_4, the enhanced downwelling branch of the residual circulation in the Northern Hemisphere (NH) middle and upper stratosphere transports more N_2O/CH_4-poor air from the upper stratosphere to the lower stratosphere. The enhanced poleward meridional branch of the residual circulation in the Southern Hemisphere (SH) stratosphere brings more N_2O/CH_4-rich air from lower to middle latitudes. These processes therefore contribute to the negative trends of N_2O and CH_4 in the NH lower stratosphere and the positive trends in the SH middle stratosphere. A corresponding positive trend is found for HCl in the NH, where the deep branch of the residual circulation located in the middle and upper stratosphere strengthens, bringing more HCl-rich air downward to the lower stratosphere, while the shallow branch of the residual circulation in the lower stratosphere weakens and leads to enhanced conversion of chlorine-containing source gases of different lifetimes to HCl. A reversed picture emerges in the SH, where the deep branch of the residual circulation in the middle and upper stratosphere weakens, while the shallow branch in the lower stratosphere strengthens, resulting in less HCl there. In addition, the southward shift of the upwelling branch of the residual circulation in recent decades can partly explain trace gas trends above 20 hPa, while the eddy mixing has a small effect on the trends. Understanding these contributions from different processes to the hemispheric asymmetries in trends of these trace gases can help us to evaluate more accurately future changes in stratospheric composition.

Key Points:
- Significant hemispheric asymmetries exist in stratospheric trends of N_2O, CH_4, and HCl over the period 2004–2012 due to different trends of residual circulation in the Northern and Southern Hemispheres
- The trend asymmetries in N_2O and CH_4 are opposite in sign to HCl, which is due to different stratospheric lifetimes and source gases
- The southward shift of the upwelling branch of the residual circulation and eddy mixing also contribute to the hemispheric asymmetries in trends of stratospheric trace gases

Correspondence to:
W. Tian,
wstian@lzu.edu.cn

Citation:
Han, Y., Tian, W., Chipperfield, M. P., Zhang, J., Wang, F., Sang, W., et al. (2019). Attribution of the hemispheric asymmetries in trends of stratospheric trace gases inferred from Microwave Limb Sounder (MLS) measurements. *Journal of Geophysical Research: Atmospheres*, *124*, 6283–6293. https://doi.org/10.1029/2018JD029723

Received 26 SEP 2018
Accepted 10 MAY 2019
Accepted article online 30 MAY 2019
Published online 24 JUN 2019

Author Contributions:
Conceptualization: Feiyang Wang
Data curation: Yuanyuan Han, Martyn P. Chipperfield, Wuhu Feng, Andreas Chrysanthou
Formal analysis: Yuanyuan Han
Investigation: Yuanyuan Han
Methodology: Jiankai Zhang, Feiyang Wang, Andreas Chrysanthou
(continued)

1. Introduction

Stratospheric trace gases play a crucial role in the planetary radiation balance. Understanding long-term trends of those radiatively and chemically active species can help us more accurately evaluate climate change (Chipperfield et al., 2015; Fueglistaler, 2012; Hu et al., 2015; Thompson & Solomon, 2009; Xie et al., 2017; Zhang et al., 2016). As one of the most important trace gases in the stratosphere, ozone decreased continuously from the late 1970s to late 1990s (Solomon, 1999; WMO, 2007, 2011; Zhang et al., 2014) but is expected to recover to pre-1980 levels by the middle of 21st century due to the reduction of ozone-depleting substances following the implementation of Montreal Protocol (Solomon et al., 2016; Weatherhead & Andersen, 2006; WMO, 2007, 2011). However, several studies have revealed differences in the ozone trend between the two hemispheres (e.g.,Eckert et al., 2014 ; Nedoluha et al., 2015); that is, stratospheric ozone has been increasing in the Southern Hemisphere (SH) midstratosphere after 2000 but still has an evident downward trend in the Northern Hemisphere (NH). Besides ozone, other stratospheric trace gases, such as CFC-11, CFC-12, and HCFC-22, have also exhibited significant hemispheric asymmetric trends in the recent decades (Chirkov et al., 2016; Haenel et al., 2015; Harrison et al., 2016; Kellmann et al., 2012; Mahieu et al., 2014; Youn et al., 2006). Youn et al. (2006) analyzed the trends of long-lived trace gases in the extratropical midstratosphere and found that in the NH hydrogen fluoride (HF) and water vapor

Project administration: Jiali Luo, Hongying Tian
Software: Jiankai Zhang
Supervision: Wenshou Tian
Validation: Jiankai Zhang, Feiyang Wang, Wenjun Sang
Writing - original draft: Yuanyuan Han
Writing – review & editing: Wenshou Tian, Martyn P. Chipperfield, Jiali Luo, Wuhu Feng, Hongying Tian

(H_2O) increased more significantly than in the SH, while stratospheric methane (CH_4) increased more significantly in the SH than in the NH. More recently, Mahieu et al. (2014) showed that hydrogen chloride (HCl) exhibited a positive trend in the NH lower stratosphere but a negative trend in the SH lower stratosphere after 2005.

Several studies have probed the possible processes responsible for this hemispheric asymmetry in the linear trends of stratospheric trace gases. Some studies have found that the stratospheric age of air (AoA) increases in the NH and decreases in the SH for the period 2002–2012, implying that the asymmetry in trend of AoA is caused mainly by the residual circulation (e.g., Haenel et al., 2015; Konopka et al., 2015; Ploeger, Abalos, et al., 2015; Ploeger, Riese, et al., 2015; Stiller et al., 2012). Youn et al. (2006) pointed out that the stronger residual circulation in the NH compared to the SH leads to the hemispheric asymmetries in trends of HF, CH_4, and H_2O. In addition, some other studies have argued that the hemispheric asymmetric changes in the residual circulation lead to an ozone return date in the NH earlier than that in the SH by 10 years (e.g., Austin et al., 2010; Eyring et al., 2010). Subsequently, Mahieu et al. (2014) further pointed out that changes in the residual circulation are responsible for the hemispheric asymmetric trend of HCl in the stratosphere. They proposed that a slowdown in the NH atmospheric circulation results in more aged air in the NH lower stratosphere; thus, there is more time for conversion of chlorine source gases to HCl to occur, contributing to the positive trend of HCl.

The above mentioned studies highlight the role of the residual circulation changes in causing the hemispheric asymmetries in trends of stratospheric trace gases. However, some studies have argued that the residual circulation makes a minor contribution to these hemispheric asymmetric trends and that the horizontal mixing process is more important. For example, Eckert et al. (2014) pointed out that a shift of the subtropical mixing barriers by 5° to the south could cause asymmetric hemispheric trends in stratospheric trace gases. Subsequently, Stiller et al. (2017) attributed the asymmetric trends of AoA and trace gases to a southward shift of the circulation pattern. In addition, Ploeger, Riese, et al. (2015) and Ploeger, Abalos, et al. (2015) showed that the integrated effects of eddy mixing and the residual circulation changes can better explain the asymmetric hemispheric trend of the stratospheric mean AoA.

It is apparent that the factors responsible for hemispheric asymmetries in trends of stratospheric trace gases in the recent decades are still under debate and several factors, including the residual circulation, eddy mixing, and the positional change of circulation pattern, are all reported to have contributed to the asymmetries. However, the relative importance of those factors remains unclear. In this study, we reexamine the trends of several stratospheric trace gases for the period from August 2004 to December 2012 and the various factors or processes that influence the hemispheric asymmetries are quantitatively evaluated. The outline of the paper is as follows: Section 2 gives a brief description of data and methods. The trends of stratospheric trace gases and the impacts of dynamical processes on them are analyzed in section 3. Conclusions are given in section 4.

2. Data Description and Methods

The primary trace gas data set used in this study is the version 4.2x Aura Microwave Limb Sounder (MLS) Level 2 data (https://acdisc.gesdisc.eosdis.nasa.gov/data/Aura_MLS_Level2/; Livesey et al., 2016), covering the period from August 2004 to December 2012. MLS measures atmospheric chemical species daily with a global coverage from 82°N to 82°S and a vertical resolution of ~3 km (Schoeberl et al., 2006). We use the gridded MLS data at a 4° latitude × 5° longitude resolution, and the quality screening rules for this data set are described by Livesey et al. (2016), who also pointed out that the MLS HCl (N_2O) product below 5 hPa (0.46 hPa) can be used for trend analysis. The 3-D winds and temperature fields used in this study are from the European Centre for Medium-Range Weather Forecasts ERA-Interim reanalysis data set (http://apps.ecmwf.int/datasets/), which has a horizontal resolution of 1° latitude × 1° longitude. More details of ERA-Interim reanalysis data can be found in Dee et al. (2011). We use a three-dimensional offline chemical transport model (SLIMCAT; Chipperfield, 2006) to analyze the hemisphere asymmetric trends of stratospheric trace gases and to diagnose the effect of eddy mixing on these trends. The SLIMCAT model has been shown to have a good representation of stratospheric chemistry and transport processes (Chipperfield, 2006; Feng et al., 2007). In this study, SLIMCAT simulations are performed at a horizontal resolution of 5.625° latitude × 5.625° longitude and driven by 6-hourly ERA-Interim reanalysis.

The Transformed Eulerian-Mean is used to accurately diagnose the relative contribution of the residual circulation and eddy mixing to the hemispheric asymmetries in trends of stratospheric trace gases. In spherical geometry, the Transformed Eulerian-Mean zonal-mean tracer continuity equations is (Abalos et al., 2013; Monier & Weare, 2011; Zhang et al., 2017)

$$\frac{\partial \overline{\chi}}{\partial t} = -\overline{v}^* \frac{\partial \overline{\chi}}{\partial \varphi} - \overline{\omega}^* \frac{\partial \overline{\chi}}{\partial z} \tag{1}$$

$$-\frac{1}{\rho_0} \nabla \cdot \boldsymbol{M} \tag{2}$$

$$+\overline{S} \tag{3}$$

Here, $\overline{\chi}$ is the tracer mixing ratio, $\overline{v}^*$ and $\overline{\omega}^*$ are the meridional and vertical velocities of the residual circulation (Andrews et al., 1987), respectively. $\boldsymbol{M}$ is the eddy flux vector $\left(\rho_0\left(\overline{v'\chi'} - \frac{\overline{v'\theta'}}{\overline{\theta}_z}\frac{\partial \overline{\chi}}{\partial z}\right), \rho_0\left(\overline{w'\chi'} + \frac{1}{R}\frac{\overline{v'\theta'}}{\overline{\theta}_z}\frac{\partial \overline{\chi}}{\partial \varphi}\right)\right)$. In this equation, overbars denote zonal means and primes are deviations from the zonal mean of a given variable. φ is latitude, z is height, ρ_0 is the air density, θ is potential temperature, R is Earth's radius, and v and w are meridional and vertical velocities, respectively. $\overline{S}$ is the net chemical production (production − loss).

To analyze the strength of the residual circulation, the residual mean mass flux is calculated from the mass stream function following the method in previous studies (e.g.,Austin et al., 2003 ; Hu et al., 2014 ; Li et al., 2010). The residual mean mass flux is defined as $F_m = 2\pi a\psi/g$, where ψ is the residual stream function given by $\frac{\partial \psi}{\partial \varphi} = -a\cos\varphi\overline{\omega}^*$ and $\frac{\partial \psi}{\partial p} = \cos\varphi\overline{v}^*$ (Austin et al., 2003).

In the following, all anomalies are defined as the deviations of a given variable from its seasonal cycle unless otherwise stated. The climatology of the variable is averaged over the period from August 2004 to December 2012.

3. Hemispheric Asymmetries in the Trends of Trace Gases

Figure 1 (left panels) shows the climatological distributions of three trace gases (N_2O, CH_4, and HCl) from August 2004 to December 2012. The linear trends of these three species are also shown in the right panels. The results for N_2O and HCl are derived from both MLS satellite measurements and the SLIMCAT simulation, whereas those for CH_4 (not observed by MLS) are only from the SLIMCAT simulation. Both the climatological distribution and linear trends of N_2O and HCl derived from the SLIMCAT simulation are in overall agreement with those derived from MLS satellite measurements, though the magnitudes are slightly different. This indicates that the hemispheric asymmetries in the trace gas trends are also captured in the model simulation. The climatological zonal-mean N_2O, CH_4, and HCl concentrations have similar distributions with isopleths bulging from the pole to the equator. In particular, the vertical and meridional gradients of N_2O and CH_4 are similar (Figures 1a, 1c, and 1d) but are opposite to those of HCl (Figures 1b and 1e).

The linear trends of these trace gases exhibit significant hemispheric asymmetries, particularly in the middle-latitude lower and middle stratosphere, with negative trends in N_2O and CH_4 in the NH lower stratosphere and positive trends in the SH middle stratosphere (Figures 1f, 1h, and 1i). Consistent with the results of Mahieu et al. (2014), HCl exhibits a positive trend in the NH lower stratosphere and a negative trend in the SH middle stratosphere (Figures 1g and 1j). The reason why N_2O and CH_4 trends in the lower and middle stratosphere have the opposite hemispheric asymmetric features to HCl is discussed below. The region with pronounced negative trends of HCl in the SH is located at 24–32 km with a maximum trend of −0.036 ppbv/yr, while the region with a pronounced positive NH HCl trend is lower, at 20–28 km, with a maximum trend of 0.019 ppbv/yr (Figure 1g). The variations of the N_2O trend in the stratosphere are in accord with those reported by Nedoluha et al. (2015; Figures 1f and 1i), with a maximum positive trend of 5.95 ppbv/yr in the SH and a maximum negative trend of −4.08 ppbv/yr in the NH (Figure 1f). In addition, the modeled CH_4 trends for the period from August 2004 to December 2012 exhibit a similar spatial pattern

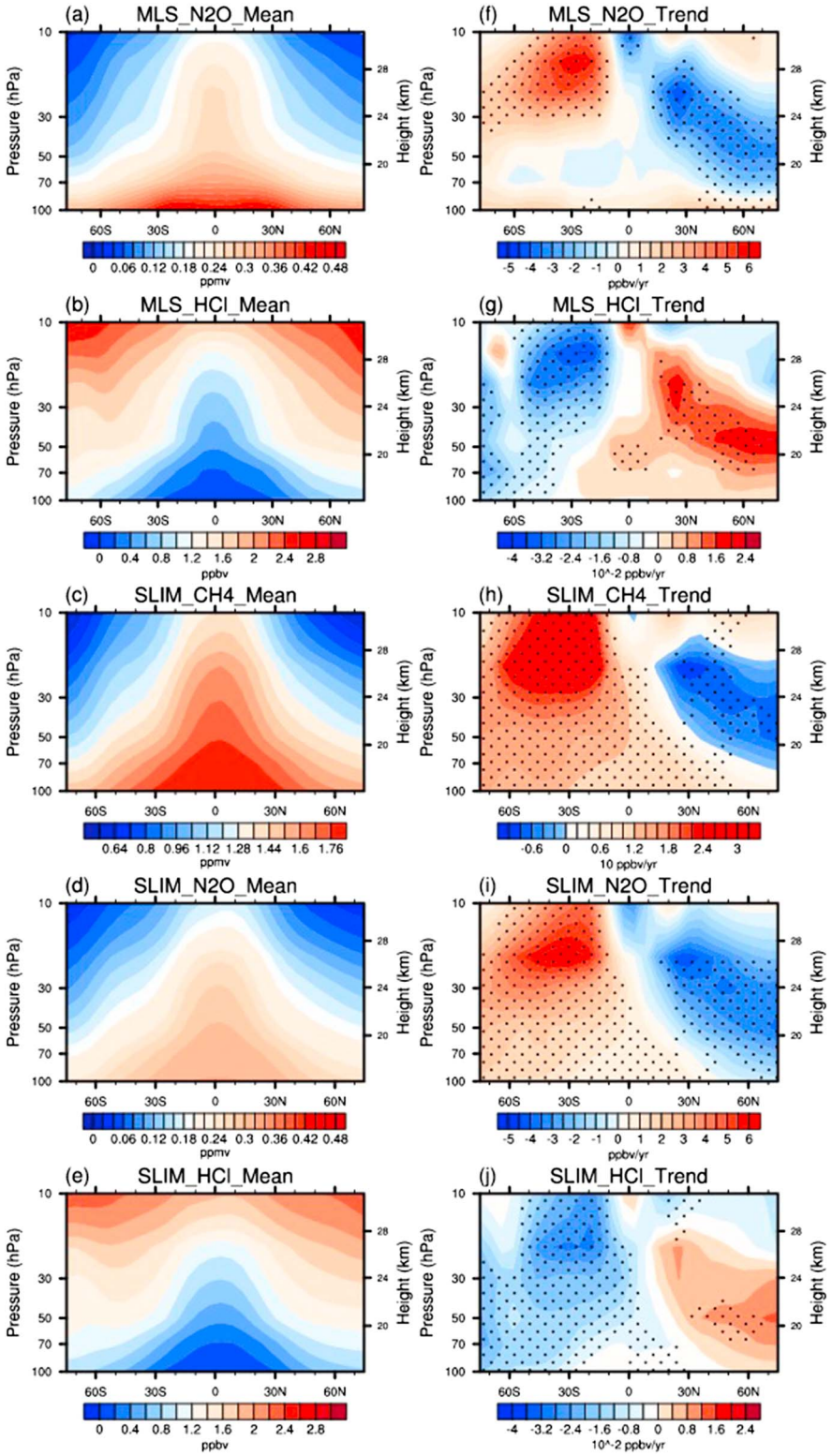

Figure 1. Latitude-height cross sections of the zonal-mean climatological distribution of (a, d) N_2O, (b, e) HCl, and (c) CH_4 for the period from August 2004 to December 2012. The corresponding latitude-height cross sections of zonal-mean linear trends of (f, i) N_2O, (g, j) HCl, and (h) CH_4 are also shown. Note that the results from both the MLS measurements and modeled N_2O and HCl are presented here for comparison (see the legends on each panel), while the results for CH_4 (not observed by the MLS) are from the SLIMCAT simulation only. The trends over stippled regions are significant at the 99% confidence level (Student's *t* test).

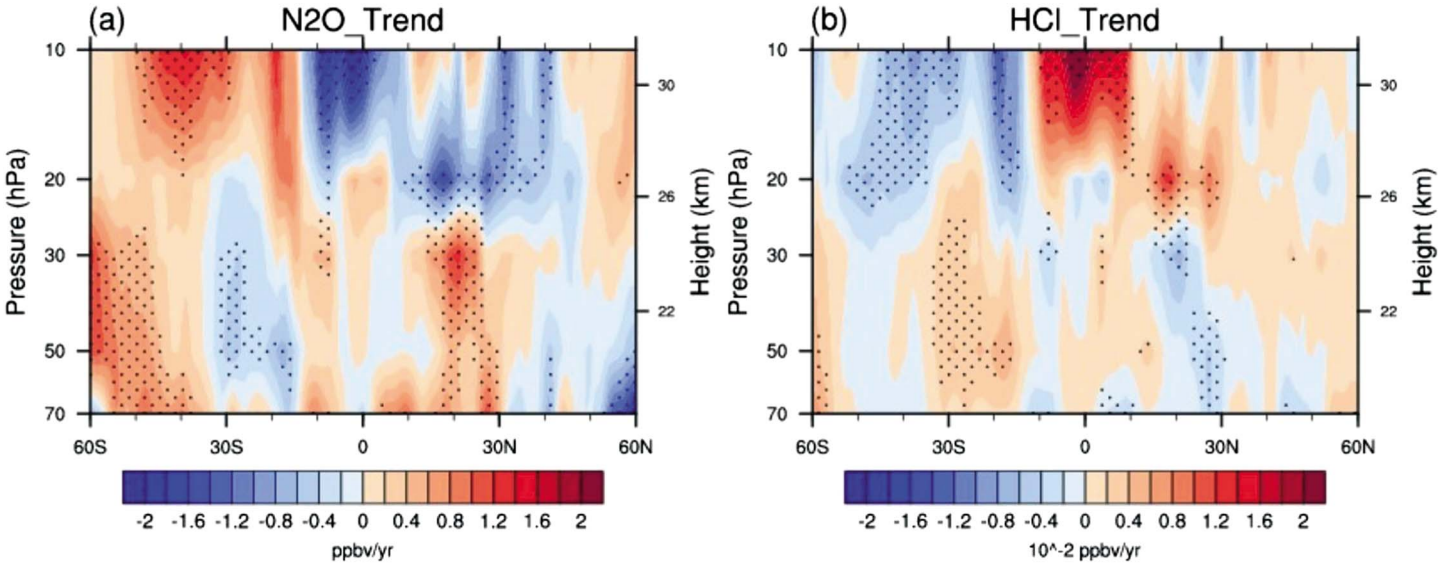

Figure 2. Linear trends of (a) N_2O and (b) HCl caused by the residual circulation for the period from August 2004 to December 2012. The trends over stippled regions are significant at the 90% confidence level (Student's *t* test).

to that of N_2O; the maximum positive trend in the SH is 32.16 ppbv/yr, and the maximum negative trend in the NH is −10.18 ppbv/yr (Figure 1h).

The residual circulation plays an important role in the distribution of trace gases in the stratosphere. Therefore, we first diagnose the influence of the residual circulation on trace gas distributions using equation (1) by considering only the advection term. Figure 2 illustrates the effect of the residual circulation on the linear trends of N_2O and HCl from August 2004 to December 2012. We choose N_2O and HCl fields to diagnose the effect of the residual circulation as these two trace gases have opposite hemispheric asymmetries in their linear trends (Figure 1). Note that the residual circulation is a large-scale meridional circulation, so it is reasonable to use monthly mean data to capture the effect of the residual circulation on trace gases. Hence, the tracer mixing ratio used here is from the monthly MLS satellite data and other required meteorological fields are from monthly ERA-Interim reanalysis data set. It is apparent that the trends of N_2O and HCl caused by the residual circulation show similar patterns to the trends in the variations of tracer concentrations in most regions of stratosphere. That is, N_2O and HCl trends caused by the residual circulation exhibit significant hemispheric asymmetries, with negative trends in N_2O (positive trends in HCl) in the NH stratosphere and positive (negative) trends in the SH stratosphere above 30 hPa. This may indicate that in most regions, the residual circulation changes contribute to the hemispheric asymmetries in the trends of these trace gases.

The above analysis indicates that the residual circulation changes have an important effect on the hemispheric asymmetries in the trends of these trace gases. Note that N_2O and CH_4 concentrations in the middle and lower stratosphere are mainly dominated by dynamical transport of the residual circulation due to their very long stratospheric lifetimes (N_2O ~ 116 years, CH_4 ~ 152 years; SPARC, 2013). Stratospheric HCl is the dominant stratospheric reservoir of inorganic chlorine, and its abundance derives from the decomposition of many long-lived chlorine-containing source gases (Mahieu et al., 2014). The major source gases are CFC-12 (stratospheric lifetime 95.5 years), CFC-11 (57 years), CFC-113 (87 years), CCl_4 (51 years), CH_3CCl_3 (37 years), and CH_3Cl (30 years; SPARC, 2013). Thus, although the HCl variation will also be influenced by the dynamical transport due to the residual circulation, the details may be different to N_2O and CH_4 due to chemical conversion from different source gases in different altitude regions, which produce different relative tracer gradients in different regions (Figure 1). In the lower stratosphere $ClONO_2$ is also an important reservoir of stratospheric inorganic chlorine.

To clarify this, Figure 3 shows the variations of the downward mass flux anomalies due to the residual circulation at 10 hPa in the two hemispheres from August 2004 to December 2012. The downwelling branch is

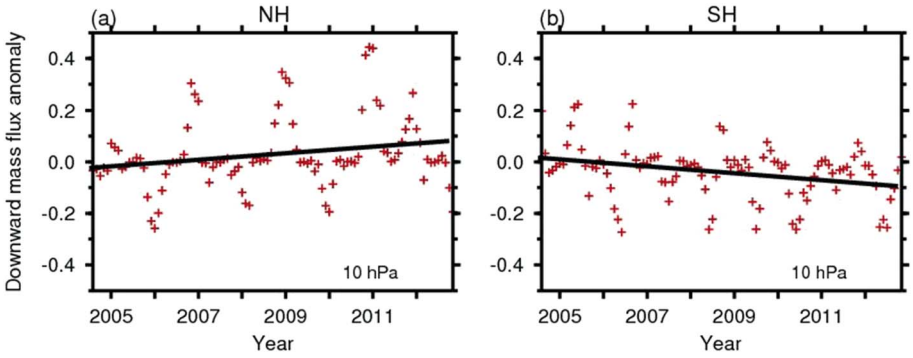

Figure 3. Variations in middle-latitude averaged downward mass flux anomalies in the (a) NH and (b) SH at 10 hPa for the period from August 2004 to December 2012. The downward mass flux at 10 hPa in the NH (SH) is calculated by integrating the 10-hPa vertical mass flux between the NH (SH) turnaround latitude and 60°N (S). The turnaround latitude in the NH (SH) is defined as the latitude where the stream function reaches its maximum (minimum), following Hardiman et al. (2014). Black lines represent trends that are significant at 90% level according to a Student's *t* test. A 3-month running mean has been applied to the original time series.

the main component of the residual circulation in middle latitudes at this altitude, so we will focus on the downward transport of the residual circulation. Here, we use the trend of downward mass flux at 10 hPa to represent the strength of the deep branch of the residual circulation (Lin & Fu, 2013). The downward mass flux due to the residual circulation at 10 hPa shows a positive trend in the NH (Figure 3a) but a negative trend in the SH (Figure 3b), suggesting that the downward branch is enhancing in the NH middle and upper stratosphere but weakening in the SH middle and upper stratosphere. With regard to N_2O and CH_4, considering their vertical gradients in the stratosphere (Figures 1a, 1c, and 1d), the stronger downward branch of the residual circulation accompanied by N_2O/CH_4-poor air transported from upper stratosphere to lower stratosphere contributes to negative trends of N_2O and CH_4 in the NH (Figures 1f, 1h, and 1i). In contrast, the weakened downward branch of the residual circulation in the SH leads to less N_2O/CH_4-poor air being transported to the lower stratosphere, contributing to the positive trends of N_2O and CH_4 in the SH (Figures 1f, 1h, and 1i). Due to the opposite vertical and meridional gradient of HCl to those of N_2O and CH_4, the dynamical transport due to the residual circulation leads to an opposite hemispheric asymmetric trend, that is, a positive trend of HCl in the NH lower stratosphere and a negative trend in the SH middle stratosphere (Figures 1g and 1j).

Figure 4a shows the latitudinal distribution of trends in meridional mass flux between 70 and 10 hPa due to the residual circulation in the NH, and Figure 4b shows the variations in the downward mass flux anomalies at 70 hPa for the period from August 2004 to December 2012. Here, we use the trend of meridional mass flux between 70 and 10 hPa and downward mass flux at 70 hPa to represent the change in strength of the shallow branch of the residual circulation, following previous studies (Hardiman et al., 2014; Lin & Fu, 2013). The

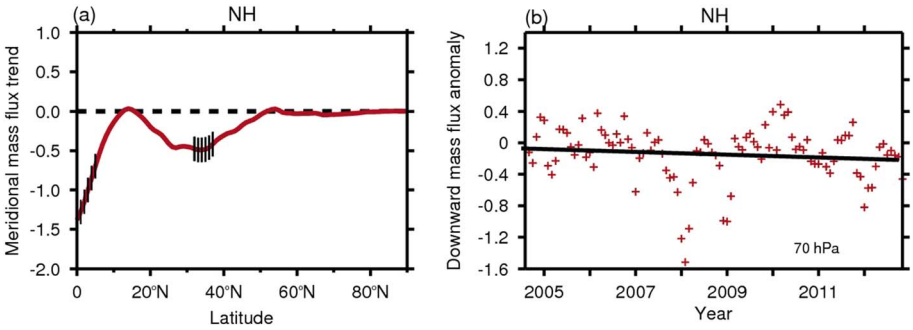

Figure 4. (a) Trends in meridional mass flux integrated over 70–10 hPa in the NH for the period from August 2004 to December 2012. The vertical bars indicate trends that are significant at the 90% confidence level (Student's *t* test). (b) Temporal evolution of downward mass flux anomalies at 70 hPa in the NH for the period from August 2004 to December 2012. The downward mass flux at 70 hPa is calculated in the same way as that at 10 hPa (see Figure 3).

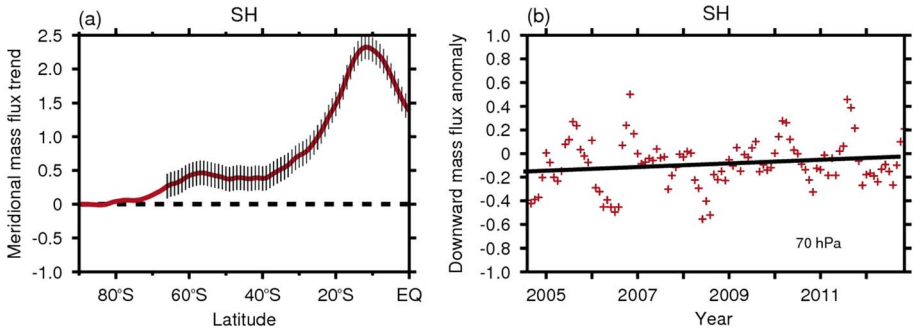

Figure 5. Same as Figure 4, but for the SH.

meridional mass flux trend in most regions of the NH stratosphere is not significant (Figure 4a), suggesting that the meridional branch of the residual circulation in the NH may not be the main factor influencing the trends of N_2O, CH_4, and HCl. Note that there is a negative trend of downward mass flux in the NH lower stratosphere (Figure 4b), implying a slowdown of the residual circulation in the lower stratosphere that is consistent with the results of Mahieu et al. (2014). The slowdown of the residual circulation leads to older AoA in the NH lower stratosphere, so that there is more time for chlorine-containing source gases to be converted to HCl. Accompanied with the HCl-rich air transported from middle and upper stratosphere to the lower stratosphere, higher HCl abundances are observed in the NH stratosphere (Figures 1g and 1j).

Figure 5 shows the trends of meridional mass flux and downward mass flux anomalies in the SH due to the residual circulation for the period from August 2004 to December 2012. The meridional mass fluxes in the lower and middle latitudes (Figure 5a) and the downward mass fluxes at 70 hPa (Figure 5b) show positive trends, implying a strengthening residual circulation in the SH lower stratosphere. The stronger meridional branch of the residual circulation in the SH enhances the transport of N_2O/CH_4-rich air from the lower latitude stratosphere to the middle- and high-latitude stratosphere, contributing to positive trends of N_2O and CH_4 in the SH stratosphere (Figures 1f, 1h, and 1i). In contrast to the NH, an acceleration of the residual circulation leads to younger AoA, so that there is less time for conversion of chlorine-containing source gases to HCl. This accompanies the weakened downward branch of the residual circulation in the SH middle and upper stratosphere resulting in less HCl-rich air being transported into the SH lower stratosphere (Figure 3b); thus, lower HCl abundances are observed (Figures 1g and 1j).

The above analysis suggests that the strength of the vertical and meridional branch of the residual circulation contributes to the hemispheric asymmetries in the trends of these trace gases. Besides the strength of the residual circulation, the width of the upwelling branch of the residual circulation can also have an impact on tracer transport in the stratosphere, so we now investigate whether the width of the upwelling branch of the residual circulation has changed from August 2004 to December 2012. Figures 6a and 6b show year-to-year variations of the turnaround latitude from 1996 to 2012 and turnaround latitude averaged over the periods 2004–2012 (red line) and 1996–2004 (black line). Time series of the annual mean turnaround latitudes in the NH and SH over the period 1996–2012 are also shown in Figure 6c. Note that there is no apparent difference in the turnaround latitudes in the lower stratosphere between the two time periods (Figures 6a and 6b). However, we find an evident southward shift of the turnaround latitude above 20 hPa in both hemispheres after 2004. In addition, the turnaround latitude averaged between 10 and 20 hPa gradually decreased in the NH and increased in the SH from 2004 to 2012 (Figure 6c). This indicates a southward shift of the upwelling branch of the residual circulation in the middle stratosphere during the period 2004–2012. This southward shift implies that air masses that are originally transported upward from the lower latitude stratosphere tend to enter the southern middle latitudes rather than the northern middle latitudes. Under such a transport condition, if a tracer has a spatial distribution like that of N_2O/CH_4 or HCl, as shown in Figure 1, there should be more air masses with high (low) concentrations of N_2O/CH_4 (HCl) being transported into the southern middle stratosphere and fewer in the northern middle stratosphere. This will contribute to the positive (negative) trends of N_2O/CH_4 (HCl) in the SH and negative (positive) trends of N_2O/CH_4 (HCl) in the NH. It is worth noting that the southward shift of the upwelling branch of the residual circulation only occurs in the middle stratosphere above 20 hPa and that this southward shift might contribute to

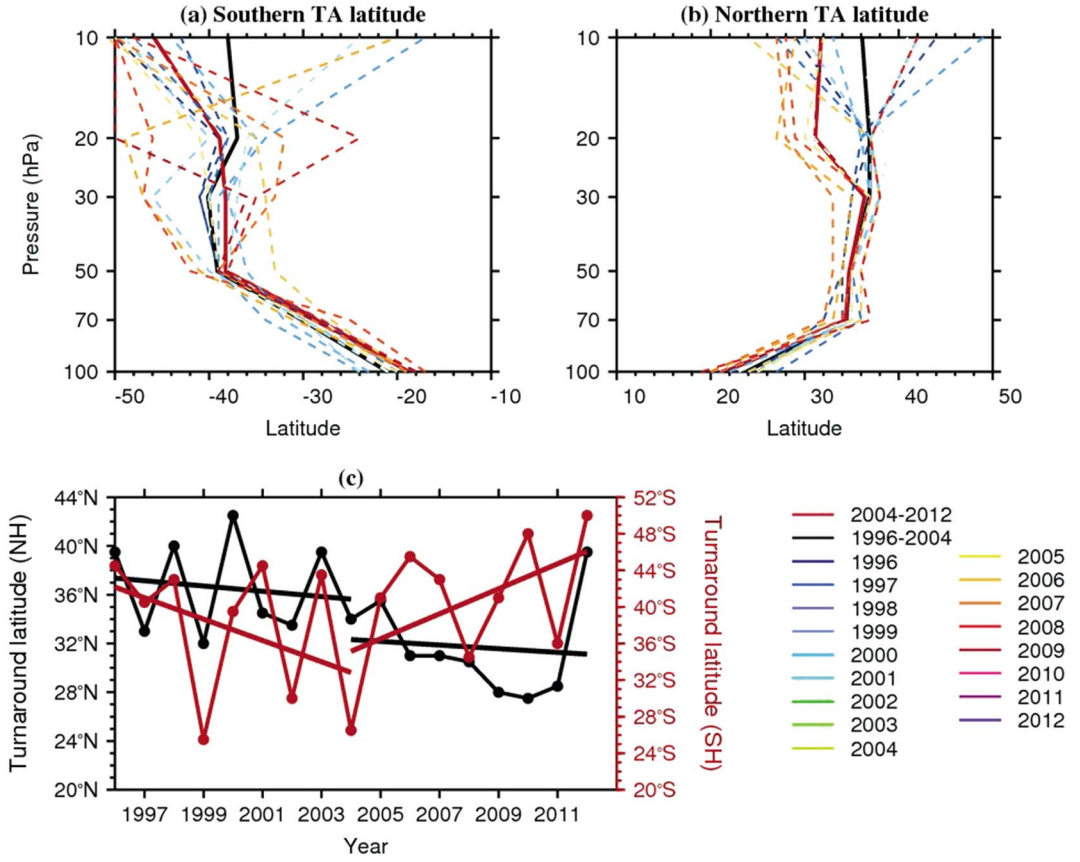

Figure 6. Variations of the turnaround latitude in the (a) Southern Hemisphere (SH) and (b) Northern Hemisphere (NH) from 1996 to 2012. Solid red and black lines represent the turnaround latitude averaged for the periods 2004–2012 and 1996–2004, respectively. (c) Time series of the annual mean turnaround latitude averaged between 10 and 20 hPa in the NH (black line) and SH (red line) for the period 1996–2012.

the trends of these trace gases in the middle stratosphere but has no significant impact on these trends in the lower stratosphere.

Eddy mixing processes can also play a role in causing the asymmetric hemispheric trends of stratospheric species; that is, eddy mixing can act on trace gas distributions by mixing air between different latitudes (Abalos et al., 2013; Monier & Weare, 2011; Ploeger, Abalos, et al., 2015; Ploeger, Riese, et al., 2015; Plumb, 2002; Riese et al., 2014). Here, by calculating according to equation (2), we diagnose the effect of eddy mixing on the distribution of trace gases during the period from August 2004 to December 2012. Similar to the analysis of the contribution of the residual circulation in the trends of trace gases, we choose N_2O and HCl fields to diagnose the eddy mixing process. Figure 7 shows the climatology and trends of eddy flux divergence for N_2O and HCl. The arrows illustrate the eddy flux vector $\boldsymbol{M}$ where we multiply the vertical component of the eddy flux vector by 200 before plotting. Note that eddy mixing is a small-scale transport process, so daily mean data derived from SLIMCAT are used here to fully capture the transport by transient eddies. To better compare with the trends in trace gases caused by the residual circulation, Figure 7 is plotted using the same contour range and color table as Figure 2. We can see from Figures 7a and 7b that the climatological distributions of eddy fluxes of both trace gases are dominated by horizontal transport and exhibit symmetric patterns in the two hemispheres. The climatological distribution of eddy N_2O fluxes (Figure 7a) is characterized by poleward eddy mixing from the lower latitude lower stratosphere, whereas that for HCl (Figure 7b) is dominated by equatorward eddy mixing from the middle- and high-latitude lower stratosphere. Therefore, eddy transport tends to decrease N_2O concentrations in the tropics by mixing N_2O-rich air from the tropics to middle and high latitudes and to increase HCl concentrations in the tropics by mixing HCl-rich air from higher latitudes.

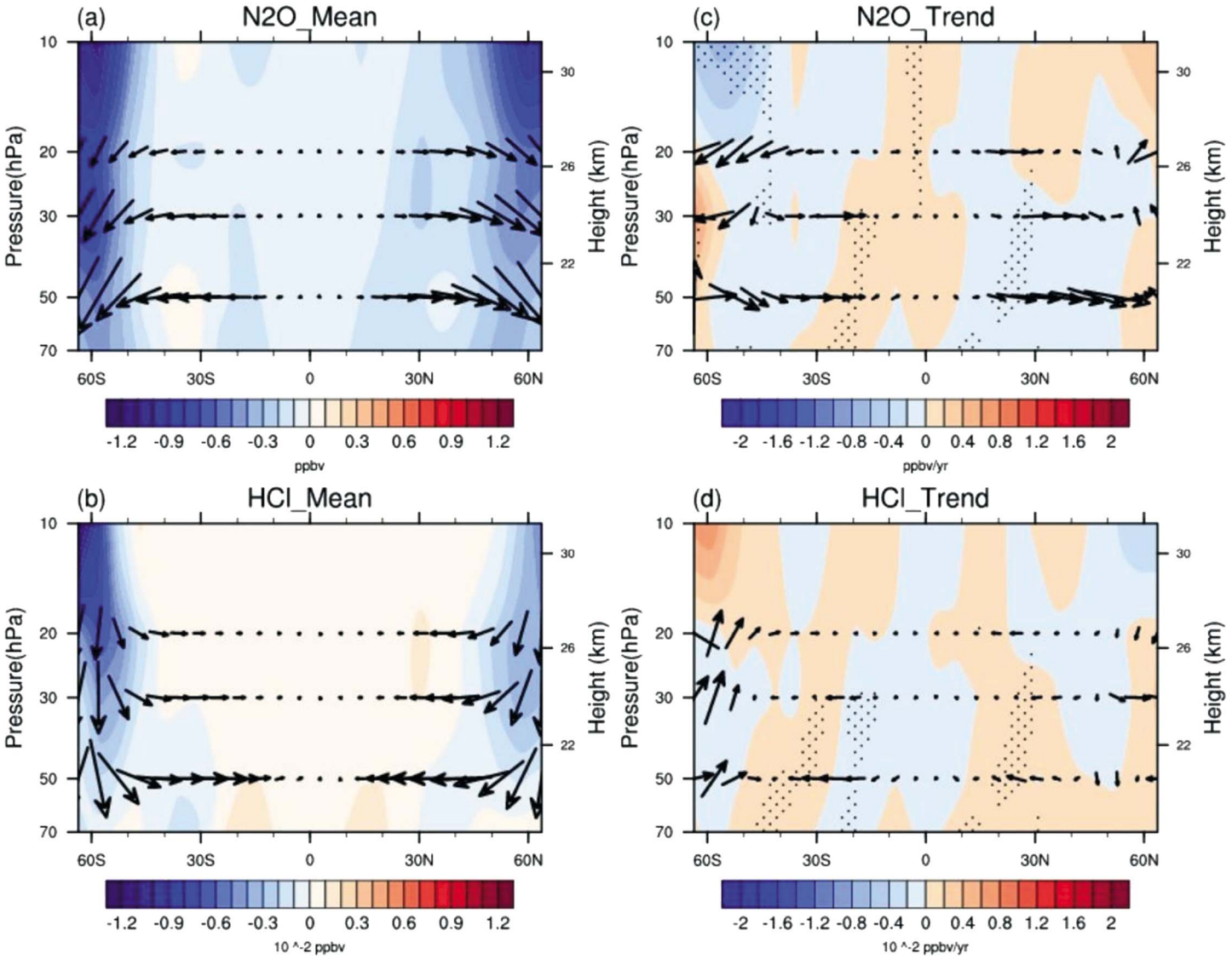

Figure 7. Climatology (left panels) and trends (right panels) of eddy flux divergence (color shading) and eddy flux vectors (arrows) for (a, c) N_2O and (b, d) HCl for the period from August 2004 to December 2012. Vertical components of the eddy flux vector have been multiplied by 200 for N_2O and HCl. The trends over stippled regions are significant at the 90% confidence level (Student's *t* test).

Clearly, the magnitudes of these trends in trace gases caused by eddy mixing (Figures 7c and 7d) are much smaller than those derived from the residual circulation (Figure 2). Eddy mixing makes a negative contribution to the N_2O trend in the high-latitude middle stratosphere in two hemispheres and in the SH middle-latitude lower stratosphere, but not in the NH middle-latitude lower stratosphere (Figure 7c). For HCl, in the high-latitude middle stratosphere (50–65°N, 10–20 hPa) and middle-latitude lower stratosphere (30–50°N, 20–70 hPa), the eddy mixing changes result in reduced HCl concentrations in the NH and increased HCl in the SH (Figure 7d), indicating that the eddy mixing process has the opposite effect on the trend of HCl to the residual circulation.

4. Conclusions

Using MLS satellite observations, ERA-Interim reanalysis data, and a 3-D chemistry transport model simulation, we have investigated the asymmetric hemispheric trends of N_2O, CH_4, and HCl during the period from August 2004 to December 2012 and diagnosed the factors responsible. The trends of these trace gases exhibit significant hemispheric asymmetries in the middle-latitude lower and middle stratosphere, with

negative trends of N_2O and CH_4 mixing ratios in the NH lower stratosphere and positive trends in the SH middle stratosphere. In contrast, HCl mixing ratios exhibit a positive trend in the northern lower stratosphere and a negative trend in the southern middle stratosphere. The opposite vertical and meridional distributions of N_2O/CH_4 and HCl are the main reason for their opposite trend asymmetries.

Our analysis suggests that the observed asymmetric hemispheric trends of stratospheric trace gases in the lower and middle stratosphere in the recent decade might be related to changes in the vertical and meridional transport due to the residual circulation. The residual circulation changes contribute to the hemispheric asymmetries in the trends of N_2O and CH_4 via dynamical transport. More specifically, the stronger deep branch of the residual circulation in the NH middle and upper stratosphere brings more N_2O/CH_4-poor air from the middle and upper stratosphere down to the lower stratosphere, and the enhanced meridional branch of the residual circulation in the SH leads to more N_2O/CH_4-rich air being transported from lower to middle and high latitude. These two processes might contribute to the negative trends of N_2O and CH_4 in the NH and the positive trends of N_2O and CH_4 in the SH. HCl is created by the chemical conversion from a number of source gases with different lifetimes, and, just as for N_2O and CH_4, the trend in HCl is caused by dynamical transport changes. In the NH, an enhanced deep branch of the residual circulation in the middle and upper stratosphere results in more HCl-rich air from middle and upper stratosphere to lower stratosphere. Meanwhile, a slowdown of the shallow branch of the residual circulation in the lower stratosphere also leads to older AoA, so that there is more time for conversion of chlorine-containing source gases of different lifetimes to HCl; thus, higher HCl abundances are observed. In contrast, a weakening deep branch of the residual circulation in the SH middle and upper stratosphere and a strengthening shallow branch of the residual circulation in the SH lower stratosphere result in less HCl-rich air and younger AoA so that lower HCl abundances are observed.

In addition, the southward shift of the upwelling branch of the residual circulation in the recent decades might partly explain the trends of these trace gases in the middle stratosphere above 20 hPa. Since the magnitudes of the trends in trace gases caused by eddy mixing are much smaller than those of the observed trends and those due to the residual circulation, we conclude that the eddy mixing has a small effect on the trends of trace gases.

Acknowledgments
The authors would like to thank the NASA for providing the Aura Microwave Limb Sounder (MLS) data (https://acdisc.gesdisc.eosdis.nasa.gov/data/Aura_MLS_Level2/) and ECMWF for providing the reanalysis data (http://apps.ecmwf.int/datasets/). The authors express their gratitude to Fei Xie for useful scientific discussions and comments. Funding for this work was provided by the National Natural Science Foundation of China under (Grants 41575038 and 41630421) and Strategic Priority Research Program of the Chinese Academy of Science under (Grant XDA17010106) and the Fundamental Research Funds for the Central Universities (lzujbky-2017-it16). SLIMCAT is supported by the UK National Centre for Atmospheric Science (NCAS).

References

Abalos, M., Randel, W. J., Kinnison, D. E., & Serrano, E. (2013). Quantifying tracer transport in the tropical lower stratosphere using WACCM. *Atmospheric Chemistry and Physics*, *13*(21), 10591–10607. https://doi.org/10.5194/acp-13-10591-2013

Andrews, D. G., Holton, J. R., & Leovy, C. B. (1987). *Middle atmosphere dynamics*, (p. 489). San Diego, Calif: Academic Press.

Austin, J., Scinocca, J., Plummer, D., Oman, L., Waugh, D., Akiyoshi, H., et al. (2010). Decline and recovery of total column ozone using a multimodel time series analysis. *Journal of Geophysical Research*, *115*, D00M10. https://doi.org/10.1029/2010jd013857

Austin, J., Shindell, D., Beagley, S. R., Brühl, C., Dameris, M., Manzini, E., et al. (2003). Uncertainties and assessments of chemistry-climate models of the stratosphere. *Atmospheric Chemistry and Physics*, *3*(1), 1–27. https://doi.org/10.5194/acp-3-1-2003

Chipperfield, M. P. (2006). New version of the TOMCAT/SLIMCAT off-line chemical transport model: Intercomparison of stratospheric tracer experiments. *Quarterly Journal of The Royal Meteorological Society*, *132*(617), 1179–1203. https://doi.org/10.1257/qj.05.51

Chipperfield, M. P., Dhomse, S. S., Feng, W., McKenzie, R. L., Velders, G. J., & Pyle, J. A. (2015). Quantifying the ozone and ultraviolet benefits already achieved by the Montreal Protocol. *Nature Communications*, *6*(1), 7233. https://doi.org/10.1038/ncomms8233

Chirkov, M., Stiller, G. P., Laeng, A., Kellmann, S., von Clarmann, T., Boone, C. D., et al. (2016). Global HCFC-22 measurements with MIPAS: Retrieval, validation, global distribution and its evolution over 2005–2012. *Atmospheric Chemistry and Physics*, *16*(5), 3345–3368. https://doi.org/10.5194/acp-16-3345-2016

Dee, D. P., Uppala, S. M., Simmons, A. J., Berrisford, P., Poli, P., Kobayashi, S., et al. (2011). The ERA-Interim reanalysis: Configuration and performance of the data assimilation system. *Quarterly Journal of The Royal Meteorological Society*, *137*(656), 553–597. https://doi.org/10.1002/qj.828

Eckert, E., von Clarmann, T., Kiefer, M., Stiller, G. P., Lossow, S., Glatthor, N., et al. (2014). Drift-corrected trends and periodic variations in MIPAS IMK/IAA ozone measurements. *Atmospheric Chemistry and Physics*, *14*(5), 2571–2589. https://doi.org/10.5194/acp-14-2571-2014

Eyring, V., Cionni, I., Bodeker, G. E., Charlton-Perez, A. J., Kinnison, D. E., Scinocca, J. F., et al. (2010). Multi-model assessment of stratospheric ozone return dates and ozone recovery in CCMVal-2 models. *Atmospheric Chemistry and Physics*, *10*(19), 9451–9472. https://doi.org/10.5194/acp-10-9451-2010

Feng, W., Chipperfield, M. P., Davies, S., von der Gathen, P., Kyrö, E., Volk, C. M., et al. (2007). Large chemical ozone loss in 2004/2005 Arctic winter/spring. *Geophysical Research Letters*, *34*, L09803. https://doi.org/10.1029/2007gl029098

Fueglistaler, S. (2012). Stepwise changes in stratospheric water vapor? *Journal of Geophysical Research*, *117*, D13302. https://doi.org/10.1029/2012jd017582

Haenel, F. J., Stiller, G. P., von Clarmann, T., Funke, B., Eckert, E., Glatthor, N., et al. (2015). Reassessment of MIPAS age of air trends and variability. *Atmospheric Chemistry and Physics*, *15*(22), 13161–13176. https://doi.org/10.5194/acp-15-13161-2015

Hardiman, S. C., Butchart, N., & Calvo, N. (2014). The morphology of the Brewer–Dobson circulation and its response to climate change in CMIP5 simulations. *Quarterly Journal of The Royal Meteorological Society*, *140*(683), 1958–1965. https://doi.org/10.1002/qj.2258

Harrison, J. J., Chipperfield, M. P., Boone, C. D., Dhomse, S. S., Bernath, P. F., Froidevaux, L., et al. (2016). Satellite observations of stratospheric hydrogen fluoride and comparisons with SLIMCAT calculations. *Atmospheric Chemistry and Physics*, *17*(17), 10501–10519. https://doi.org/10.5194/acp-17-10501-2017

Hu, D., Tian, W., Xie, F., Shu, J., & Dhomse, S. (2014). Effects of meridional sea surface temperature gradients on the stratospheric temperature and circulation. *Advances in Atmospheric Sciences*, *31*(4), 888–900. https://doi.org/10.1007/s00377-013-3152-7

Hu, D., Tian, W., Xie, F., Wang, C., & Zhang, J. (2015). Impacts of stratospheric ozone depletion and recovery on wave propagation in the boreal winter stratosphere. *Journal of Geophysical Research: Atmospheres*, *120*, 8299–8317. https://doi.org/10.1002/2014JD022855

Kellmann, S., von Clarmann, T., Stiller, G. P., Eckert, E., Glatthor, N., Höpfner, M., et al. (2012). Global CFC-11 (CCl_3F) and CFC-12 (CCl_2F_2) measurements with the Michelson Interferometer for Passive Atmospheric Sounding (MIPAS): Retrieval, climatologies and trends. *Atmospheric Chemistry and Physics*, *12*(24), 11857–11875. https://doi.org/10.5194/acp-12-11857-2012

Konopka, P., Ploeger, F., Tao, M., Birner, T., & Riese, M. (2015). Hemispheric asymmetries and seasonality of mean age of air in the lower stratosphere: Deep versus shallow branch of the Brewer-Dobson circulation. *Journal of Geophysical Research: Atmospheres*, *120*, 2053–2066. https://doi.org/10.1002/2014jd022429

Li, F., Stolarski, R. S., Pawson, S., Newman, P. A., & Waugh, D. (2010). Narrowing of the upwelling branch of the Brewer-Dobson circulation and Hadley cell in chemistry-climate model simulations of the 21st century. *Geophysical Research Letters*, *37*, L13702. https://doi.org/10.1029/2010gl043718

Lin, P., & Fu, Q. (2013). Changes in various branches of the Brewer–Dobson circulation from an ensemble of chemistry climate models. *Journal of Geophysical Research: Atmospheres*, *118*, 73–84. https://doi.org/10.1029/2012JD018813

Livesey, N. J., Read, W. G., Wagner, P. A., Froidevaux, L., Lambert, A., Manney, G. L., et al. (2016). EOS MLS Version 4.2x Level 2 data quality and description document, Rev., B, Jet Propulsion Laboratory, D-33509.

Mahieu, E., Chipperfield, M. P., Notholt, J., Reddmann, T., Anderson, J., Bernath, P. F., et al. (2014). Recent Northern Hemisphere stratospheric HCl increase due to atmospheric circulation changes. *Nature*, *515*(7525), 104–107. https://doi.org/10.1038/nature13857

Monier, E., & Weare, B. C. (2011). Climatology and trends in the forcing of the stratospheric ozone transport. *Atmospheric Chemistry and Physics*, *11*(13), 7311–7323. https://doi.org/10.5194/acp-11-7311-2011

Nedoluha, G. E., Boyd, I. S., Parrish, A., Gomez, R. M., Allen, D. R., Froidevaux, L., et al. (2015). Unusual stratospheric ozone anomalies observed in 22 years of measurements from Lauder, New Zealand. *Atmospheric Chemistry and Physics*, *15*(12), 7817–7827. https://doi.org/10.5194/acp-15-7817-2015

Ploeger, F., Abalos, M., Birner, T., Konopka, P., Legras, B., Müller, R., & Riese, M. (2015). Quantifying the effects of mixing and residual circulation on trends of stratospheric mean age of air. *Geophysical Research Letters*, *42*, 2047–2054. https://doi.org/10.1002/2014gl072927

Ploeger, F., Riese, M., Haenel, F., Konopka, P., Müller, R., & Stiller, G. (2015). Variability of stratospheric mean age of air and of the local effects of residual circulation and eddy mixing. *Journal of Geophysical Research: Atmospheres*, *120*, 717–733. https://doi.org/10.1002/2014JD022478

Plumb, R. A. (2002). Stratospheric transport. *Journal of the Meteorological Society of Japan*, *80*(4B), 793–809. https://doi.org/10.2151/jmsj.80.793

Riese, M., R. Mueller, G. Stiller, P. Konopka, and F. Ploeger (2014), On the relationship between age-of-air (AoA) changes and changes in residual circulation and eddy mixing, 40th COSPAR Scientific Assembly, 40.

Schoeberl, M. R., Douglass, A. R., Hilsenrath, E., Bhartia, P. K., Beer, R., Waters, J. W., et al. (2006). Overview of the EOS aura mission. *IEEE Transactions on Geoscience and Remote Sensing*, *44*(5), 1066–1074. https://doi.org/10.1109/TGRS.2005.861950

Solomon, S. (1999). Stratospheric ozone depletion: A review of concepts and history. *Reviews of Geophysics*, *37*(3), 275–316. https://doi.org/10.1029/1999RG900008

Solomon, S., Ivy, D. J., Kinnison, D., Mills, M. J., Neely, R. R., & Schmidt, A. (2016). Emergence of healing in the Antarctic ozone layer. *Science*, *353*.

SPARC (2013). SPARC report on the lifetimes of stratospheric ozone-depleting substances, their replacements, and related species, M. Ko, P. Newman, S. Reimann, S. Strahan (Eds.), SPARC Report No. 6, WCRP-15/2013.

Stiller, G. P., Fierli, F., Ploeger, F., Cagnazzo, C., Funke, B., Haenel, F. J., et al. (2017). Shift of subtropical transport barriers explains observed hemispheric asymmetry of decadal trends of age of air. *Atmospheric Chemistry and Physics*, *17*(18), 11177–11192. https://doi.org/10.5194/acp-17-11177-2017

Stiller, G. P., von Clarmann, T., Haenel, F., Funke, B., Glatthor, N., Grabowski, U., et al. (2012). Observed temporal evolution of global mean age of stratospheric air for the 2002 to 2010 period. *Atmospheric Chemistry and Physics*, *12*(7), 3311–3331. https://doi.org/10.5194/acp-12-3311-2012

Thompson, D. W. J., & Solomon, S. (2009). Understanding recent stratospheric climate change. *Journal of Climate*, *22*(8), 1934–1943. https://doi.org/10.1175/2008jcli2482.1

Weatherhead, E. C., & Andersen, S. B. (2006). The search for signs of recovery of the ozone layer. *Nature*, *441*(7092), 518–522. https://doi.org/10.1038/nature04747.

WMO (2007). *Scientific assessment of ozone depletion: 2007*, Rep. 50, *Global Ozone Res. and Monit, Project*. Switzerland: Geneva.

WMO (2011). *Scientific assessment of ozone depletion: 2010*, Rep. 52, *Global Ozone Res. and Monit. Project* (p. 517). Switzerland: Geneva.

Xie, F., Li, J., Zhang, J., Tian, W., Hu, Y., Zhao, S., et al. (2017). Variations in North Pacific sea surface temperature caused by Arctic stratospheric ozone anomalies. *Environmental Research Letters*, *12*(11). https://doi.org/10.1088/1748-9326/aa9005

Youn, D., Choi, W., Lee, H., & Wuebbles, D. J. (2006). Interhemispheric differences in changes of long-lived tracers in the middle stratosphere over the last decade. *Geophysical Research Letters*, *33*, L03807. https://doi.org/10.1029/2005GL024274

Zhang, J., Tian, W., Chipperfield, M., Xie, F., & Huang, J. (2016). Persistent shift of the Arctic polar vortex towards the Eurasian continent in recent decades. *Nature Climate Change*, *6*(12), 1094–1099. https://doi.org/10.1038/nclimate3136

Zhang, J., Tian, W., Xie, F., Tian, H., Luo, J., Zhang, J., et al. (2014). Climate warming and decreasing total column ozone over the Tibetan Plateau during winter and spring. *Tellus*, *77*(0). https://doi.org/10.3402/tellusb.v77.23415

Zhang, J., Xie, F., Tian, W., Han, Y., Zhang, K., Qi, Y., et al. (2017). Influence of the Arctic Oscillation on the vertical distribution of wintertime ozone in the stratosphere and upper troposphere over Northern Hemisphere. *Journal of Climate*. https://doi.org/10.1175/JCLI-D-16-0651